



ELSEVIER

Journal of Crystal Growth 166 (1996) 779–785

JOURNAL OF
**CRYSTAL
GROWTH**

Heteroepitaxial growth of TiO_2 films by ion-beam sputter deposition

P.A. Morris Hotsenpiller^{a,*}, G.A. Wilson^a, A. Roshko^b, J.B. Rothman^c,
G.S. Rohrer^d

^a DuPont Company, Experimental Station, Wilmington, Delaware 19880-0356, USA

^b National Institute of Standards and Technology, Boulder, Colorado 80303-3328, USA

^c Laboratory for Research on the Structure of Matter, University of Pennsylvania, Philadelphia, Pennsylvania 19104, USA

^d Department of Materials Science and Engineering, Carnegie Mellon University, Pittsburgh, Pennsylvania 15213, USA

Abstract

Heteroepitaxial TiO_2 films of the rutile and anatase phases have been grown using the ion-beam sputter deposition technique. The orientations of the highest-quality rutile films grown and their corresponding substrates are (100)/(0001) Al_2O_3 , (101)/(11 $\bar{2}$ 0) Al_2O_3 , (001)/(10 $\bar{1}$ 0) Al_2O_3 , and (110)/(110) MgO . This is the first report of the heteroepitaxial growth of (001)/(10 $\bar{1}$ 0) Al_2O_3 and (110)/(110) MgO rutile films. Results indicate that the films are aligned both perpendicular and parallel to the plane of the film. Distinct surface morphologies are observed for each orientation. The (100) and (101) rutile orientations were also grown on (111) MgO and (1 $\bar{1}$ 02) Al_2O_3 , respectively. The (100) anatase grew on both (100) MgO and MgAl_2O_4 . The growth mechanisms of several rutile films on Al_2O_3 substrates were investigated, and the data suggest island or Volmer–Weber type growth.

1. Introduction

Crystalline TiO_2 thin films are of interest for use in a range of applications including photocatalysts for wastewater treatment and solar-energy conversion, storage capacitors in DRAMs, insulators in MOS devices, electrochromic displays, gas sensors, waveguides, and other optical coatings. The optical and surface properties of TiO_2 provide for the variety of potential devices. This interest has spawned research into growth techniques for producing heteroepitaxial TiO_2 films. Thus far, heteroepitaxial TiO_2 has only been grown in situ using chemical vapor deposition (CVD) techniques with a TiCl_4

precursor [1,2], metalorganic chemical vapor deposition (MOCVD) with $\text{Ti}(\text{OC}_3\text{H}_7)_4$ as the precursor [3–6], and the reactive ionized cluster beam (RICB) technique [7–9]. Several orientations of the high-temperature rutile and low-temperature anatase phases have been grown using these techniques.

In this paper, we report the results of our research on the growth of heteroepitaxial TiO_2 films using ion-beam sputter deposition with a variety of substrates. Ion-beam techniques are commonly used to produce amorphous TiO_2 optical coatings [10]. The purpose of our work is to produce high-quality, heteroepitaxial TiO_2 films of the surface orientations of the rutile and anatase phases for use in photocatalytic applications. A companion paper discusses related work on developing a solid-source MOCVD process for the growth of TiO_2 films [11].

* Corresponding author.

2. Experimental procedure

The films were grown using an ion-beam sputtering system developed to produce complex oxide thin films. This system has previously been used to grow heteroepitaxial nonlinear optical films, such as KNbO_3 [12]. The chamber was evacuated to 1×10^{-7} Torr prior to deposition. Substrates were introduced into the system through a load-lock chamber. The substrate stage was heated by halogen lamps, and the temperature was monitored by a thermocouple and an infrared pyrometer. Deposition resulted from reactively sputtering a high-purity (99.995%) Ti target with a Xe ion beam from a 3 cm Kaufmann-type ion source. The ion-beam energy and current were 1000 eV and 20 mA, respectively. The growth atmosphere consisted of 1×10^{-4} Torr of Xe and 1×10^{-4} Torr of O_2 . Films were grown at substrate temperatures from 450 to 725°C. The growth rate was 3 \AA min^{-1} . Films were typically grown with thicknesses in the range of 700–4500 Å.

The substrates used in this work include (0001), (11 $\bar{2}$ 0), (10 $\bar{1}$ 0), and (1 $\bar{1}$ 02) Al_2O_3 ; (100), (110), and (111) MgO ; (100) MgAl_2O_4 ; (100) Si; (10 $\bar{1}$ 0) quartz; fused quartz, and microscope-slide glass. All crystalline substrates used were epitaxially polished by the suppliers. Prior to introduction into the vacuum

chamber, the substrates were rinsed with high-purity methanol. MgO substrates had to be kept under vacuum while being stored to prevent the formation of hydroxides on their surfaces. All substrates were kept in dryboxes prior to use.

The ratio of Ti to oxygen and the thickness were measured using Rutherford backscattering spectrometry (RBS) of 2 MeV $^4\text{He}^+$ ions. The crystalline structure of the films was checked by X-ray diffraction with $\text{Cu K}\alpha$ radiation and RBS channeling. Their surface roughness and morphology were examined by atomic force microscopy (AFM) and scanning electron microscopy (SEM).

3. Results and discussion

3.1. Structural properties

RBS measurements were used to determine the Ti:O stoichiometry of the films. Stoichiometric TiO_2 films were grown at all temperatures with the chamber oxygen pressure at 1×10^{-4} Torr. The crystalline structure of the films was examined by X-ray diffraction and RBS channeling. Table 1 shows the TiO_2 phases and orientations of several of the heteroepitaxial films grown with their corresponding

Table 1
Growth conditions and properties of heteroepitaxial TiO_2 films grown by ion-beam sputter deposition

Film	Substrate	Growth temperature (°C)	Thickness (Å)	FWHM (degree)	Min. yield: Ti (% film / % bulk)	Roughness RMS (Å)
(100) rutile	(0001) Al_2O_3	725	700	0.20	5/5	5–7
			2200	0.20	–	4–5
			4500	0.20	–	–
(101) rutile	(11 $\bar{2}$ 0) Al_2O_3	725	700	0.80	–	–
			2200	0.35	33/17	7–25
			4500	0.35	–	35
(001) rutile	(1 $\bar{1}$ 02) Al_2O_3	725	700	1.0	–	–
			2200	0.35	25/3	12–38
			4500	0.35	–	24–75
(110) rutile	(110) MgO	600	700	1.5	50/17	55
			2200	1.5	–	90
			4500	2.25	–	–
(100) anatase	(100) MgO	450	700	1.75	–	–
	(100) MgAl_2O_4	550	700	1.25	–	–

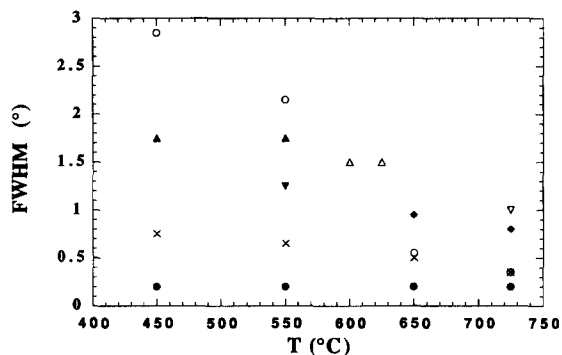


Fig. 1. The X-ray rocking curve FWHMs as a function of growth temperature for the following TiO₂ films: (●) (100) rutile/(0001)Al₂O₃, (○) (101) rutile/(11̄20)Al₂O₃, (×) (001) rutile/(10̄10)Al₂O₃, (△) (110) rutile/(110)MgO, (◆) (100) rutile/(111)MgO, (∇) (101) rutile/(1̄102)Al₂O₃, (▲) (100) anatase/(100)MgO, and (▼) (100) anatase/(100)MgAl₂O₄.

substrates. The growth conditions listed for each TiO₂ orientation are generally those which produced the highest-quality films on that substrate. The full width half maximums (FWHMs) of the X-ray rocking curves of the TiO₂ film peaks are also listed in Table 1. Fig. 1 shows the FWHMs of the rocking curves of the films as a function of growth temperature. The ratios of the RBS channeling minimum yields of Ti in the films to those obtained for bulk single-crystal rutile samples of the same orientations are shown in Table 1 for several of the highest-quality films. These results give a measure of the degree of disorder of the Ti ions in the films. In addition, RBS channeling maps of the cation scattering in these films, their substrates and similar orientations of bulk single-crystal rutile samples were determined in an angular range of $\pm 5^\circ$ from the minimum-yield positions. Comparison of the channeling maps corresponding to each film orientation allowed the in-plane film structure and the symmetry relationship of the film to the substrate to be examined.

The X-ray rocking curve FWHMs of the (100) rutile films grown on (0001)Al₂O₃ are 0.2° – the resolution of the instrument used. This is comparable to the best results obtained previously with the MOCVD and RICB techniques [6,8,9]. The FWHMs of the rocking curves are not found to be a function of the growth temperature or film thickness in the ranges investigated here (Table 1, Fig. 1). The RBS channeling minimum yield of Ti is 5%. This is equal

to the value obtained for the bulk single-crystal rutile sample and suggests that there is very little disorder in the film. The channeling maps in Fig. 2 show that the pattern and symmetry of the bulk rutile crystal, film, and substrate maps are similar, indicating that the film is aligned in the plane of the film and to the substrate structure. Single-crystal heteroepitaxial films of this orientation on (0001)Al₂O₃ were previously reported using the RICB technique [9]. The quality of these films is somewhat surprising given the large lattice mismatches calculated. Depending on the coincident site lattice (CSL) method used, mismatches of (3.76 and 7.27%) and (3.59 and 8.03%) have been obtained for this film/substrate system [6,8,9]. The (100) rutile films were also grown on (111)MgO substrates from 650 to 725°C. The minimum rocking curve (0.8°) was observed for the film grown at 725°C.

The (101) rutile films grown at 725°C on (11̄20)Al₂O₃ have 0.35° rocking curves. The FWHMs of the rocking curves are comparable to those obtained previously for this film orientation and substrate [3,4,9]. The rocking curve widths do not appear to be a function of the thickness of the film, up to 4500 Å. However, the widths of the rocking curves of the films do increase as the growth temperature is lowered (Fig. 1), as observed in Ref. [6]. The RBS% minimum yield of the 725°C film is 33%, which is approximately two times that of the bulk crystal sample. This indicates that there is some disorder on the Ti sublattice in the film. However, the RBS channeling map of the film has a similar pattern and symmetry to that of the bulk single-crystal rutile, suggesting that the in-plane structure of the film is highly oriented. Single crystal films of this orientation have reportedly been grown before on (11̄20)Al₂O₃ using both the MOCVD and RICB techniques [3,4,9]. The channeling minimum and symmetry pattern of the film map are offset by approximately $2\text{--}3^\circ$ from those of the substrate, indicating that (101) rutile prefers to grow “tilted” slightly off-axis under these conditions on (11̄20)Al₂O₃. Earlier work using the MOCVD technique showed that the (100) rutile orientation preferred to grow when this substrate was cut 3° off-axis [5]. Both of these observations indicate that a specific matching of the ions at this film/substrate interface is necessary for heteroepitaxial growth to

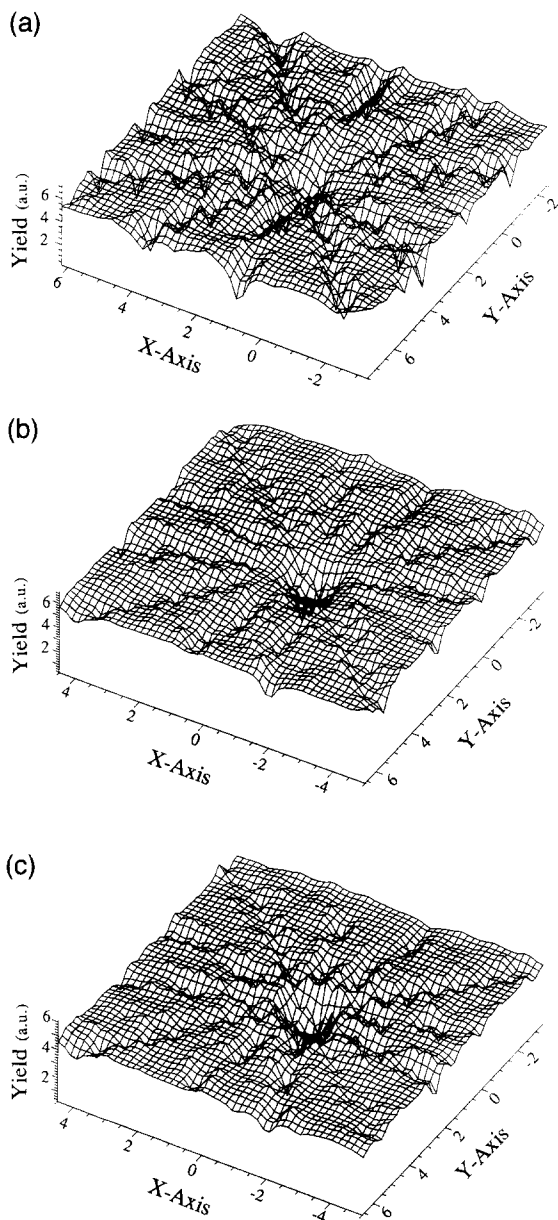


Fig. 2. RBS channeling maps showing the channeling yield in arbitrary units (a.u.) versus the angular tilt of the sample around the x and y axes for (a) single-crystal bulk (100) rutile, (b) the (100) rutile film (700 Å thick), and (c) the (0001) Al_2O_3 substrate. The channeling maps were produced by monitoring the cation scattering efficiencies. The film and substrate maps were taken simultaneously.

occur. Some variability in the results were observed for growth on (11 $\bar{2}$ 0) Al_2O_3 substrates processed at different times, possibly due to the substrates being

cut slightly off-axis. The CSL mismatches reported, (0.91 and 5.78%) [9] and (0.5 and 5.9%) [3,4], are smaller than those calculated for the (100) rutile/(0001) Al_2O_3 films, but are still rather large in one direction. The (101) rutile orientation could also be grown on (1 $\bar{1}$ 02) Al_2O_3 substrates from 450 to 725°C, but the minimum rocking curve (1° at 725°C) was larger than that obtained for films grown on the (11 $\bar{2}$ 0) orientation.

Rutile films with the (001) orientation were grown on (10 $\bar{1}$ 0) Al_2O_3 substrates. This is the first report of the heteroepitaxial growth of the (001) rutile orientation. The films grown at 725°C have an X-ray rocking curve of 0.35°, which is constant over the range of thicknesses grown. The rocking curves do gradually increase with decreasing growth temperatures (Fig. 1). The RBS% minimum yield is 25%, which is considerably higher than the 3% measured on the bulk-crystal sample. However, the RBS channeling maps of the film and (001) bulk rutile crystal have similar patterns and symmetries. The results indicate that the films have a significant amount of disorder on the Ti sublattice, but that their structure is oriented in the plane of the film. The channeling minimum and symmetry pattern of the film and substrate are aligned. The CSL mismatch calculated using the lattice parameters of these orientations of rutile and Al_2O_3 are (3.6 and 5.72%), which is in the range calculated for the other films/substrates.

The (110) rutile films were grown at 600°C on (110) MgO substrates and the widths of the X-ray rocking curves of these films are 1.5°. Previously, (110) rutile films were grown on (100) MgO substrates using CVD techniques [1,2]. The X-ray rocking curves were similar [2]. While a relatively small effect of thickness is observed on the rocking curve width in the range investigated here, there is a very dramatic temperature effect. In fact, the heteroepitaxial structure of the film is only observed from 600 to 625°C. The RBS channeling minimum yield is 50%, which is approximately three times that observed for the bulk crystalline rutile sample. The RBS channeling maps of the film and single crystal rutile sample have similar patterns and symmetries, indicating that the films are aligned in the plane of the film. The RBS minimums and symmetries of the film and substrate also appear to be aligned. The CSL mismatch calculated for this film/substrate system (0.6

and 2.7%) is much smaller than those of the other films discussed. This makes the narrow temperature range of heteroepitaxial growth rather surprising. One possible explanation for this behavior is the formation of twins in the film on the {011} planes due to thermal stresses at other growth temperatures. These twins are commonly observed in bulk rutile crystals [13].

The (100) anatase orientation was grown on (100)MgO and (100)MgAl₂O₄ substrates at growth temperatures of 450–550°C and 550°C, respectively. The X-ray rocking curve FWHMs were 1.75° on MgO and 1.25° on MgAl₂O₄. Heteroepitaxial growth of the (100) orientation of anatase has not previously been reported. The (112) orientation has been grown on (0001)Al₂O₃ and glass substrates [3,4,7]. (001) anatase films were grown on (001) SrTiO₃ [6]. It is interesting that many of the rutile film orientations can be grown at temperatures below the 700°C transition temperature [14].

No heteroepitaxial growth was observed using (100) Si and (10 $\bar{1}$ 0) quartz substrates at 450–550°C

or fused quartz and microscope slide glass at 650°C. Other workers have obtained similar results using other techniques [8,15,16]. The only reported in situ, heteroepitaxial growth of either TiO₂ phase on these substrates was (112) anatase on glass [7]. The (110) rutile has been grown on (100) Si by annealing after deposition [17] and oxidizing epitaxial TiN films [18].

3.2. Surface morphologies

The surface morphologies of several of the films have been examined using AFM and SEM. The root-mean-square (RMS) values of the surface roughnesses determined from AFM are shown in Table 1 for films with thicknesses of 700 and 2200 Å. The SEM images of the surfaces of the 2200 Å thick films are shown in Fig. 3. The smoothest film is the (100) rutile/(0001)Al₂O₃. The surface roughness is 5–7 Å for the 700 Å thick film and does not increase as the film thickness increases to 2200 Å. The lack of prominent features in the surface topog-

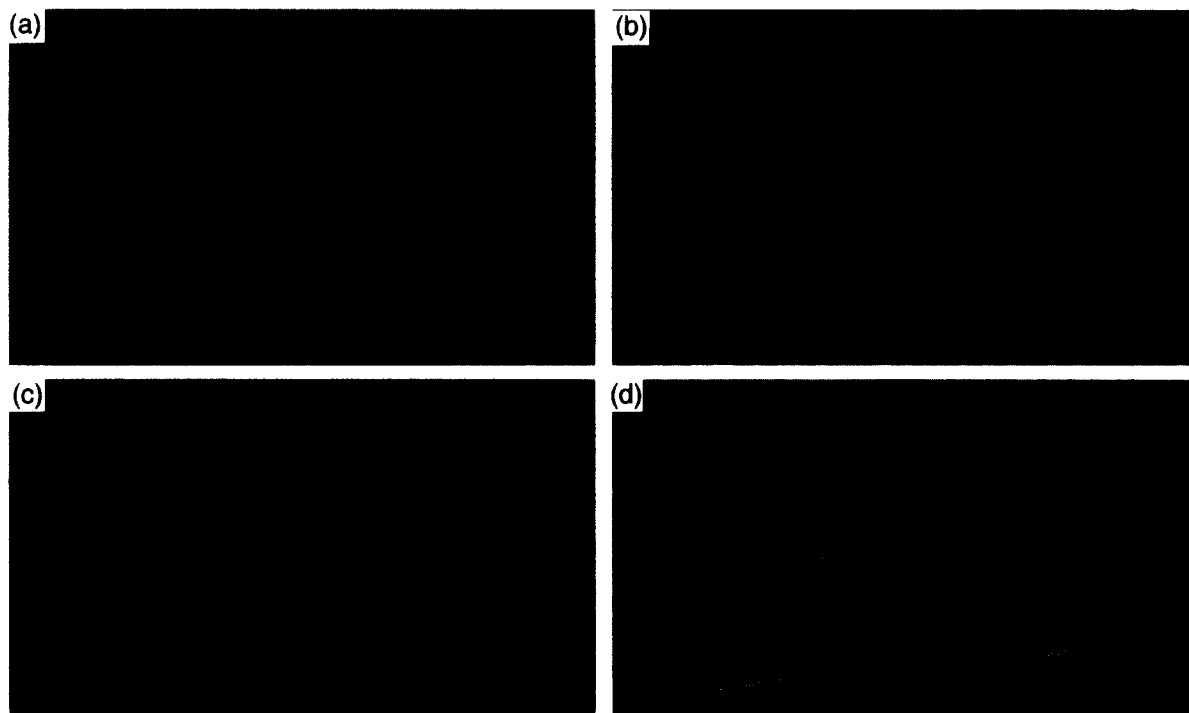


Fig. 3. SEM micrographs of the following 2200 Å thick rutile films: (a) (100)/(0001)Al₂O₃, (b) (101)/(11 $\bar{2}$ 0)Al₂O₃, (c) (001)/(10 $\bar{1}$ 0)Al₂O₃, and (d) (110)/(110)MgO. The magnification scale of the images is shown on (a).

raphy is also apparent in the SEM micrograph in Fig. 3. The (101), (001), and (110) rutile films do become rougher as they become thicker. The RMS surface roughnesses of the 2200 Å thick (101) rutile/(11 $\bar{2}$ 0)Al₂O₃, (001) rutile/(10 $\bar{1}$ 0)Al₂O₃ and (110) rutile/(110)MgO films are 35, 24–75 and 90 Å, respectively. Fig. 3 shows that each of these films has a distinct surface morphology. The (101) and (110) rutile films have significant regions of their surfaces which are quite smooth compared to the overall surface, as might be expected from the morphology of bulk rutile [13]. The (100), (101), and (110) facets occupy the majority of the surface area of bulk rutile crystals.

3.3. Growth mechanisms

The mechanisms of growth of the (100) rutile/(0001)Al₂O₃, (101) rutile/(11 $\bar{2}$ 0)Al₂O₃, and (001) rutile/(10 $\bar{1}$ 0)Al₂O₃ films grown at 725°C were investigated by examining the surface morphologies of films nominally 15 and 100 Å thick using AFM. The maximum height, RMS roughness and island diameters were characterized for each film. All of these films appear to grow via island or Volmer–Weber type growth. This growth mechanism may occur due to the relatively large interfacial energy resulting from the CSL mismatches between the tetragonal rutile and pseudo-hexagonal Al₂O₃ structures.

The island diameters observed are approximately 150 Å for all of the 15 Å thick films. The maximum heights vary in the range of 22–33 Å, and the RMS roughnesses are between 2.2 and 3.5 Å depending on the orientation. As the films get thicker, the island dimensions grow at different rates for each orientation. The islands found on the 100 Å thick, (101) rutile film were elongated (250 × 500 Å²). This growth morphology most likely results in the textured surface seen in Fig. 3. The maximum heights and RMS roughnesses of the (100) rutile films are larger than for the other orientations at both thicknesses. This may result from the larger CSL mismatch for the (100) rutile/(0001)Al₂O₃ film. In fact, at ~100 Å thickness, the maximum heights and RMS roughnesses of the films correlate with their CSL mismatches. However, by the time the films are 700–2200 Å thick, the surface roughnesses are not correlated to the lattice mismatches. Surface energies

may play a more dominant role in determining the surface morphologies as the films become thicker.

4. Conclusions

The ion-beam sputter deposition technique has been used to successfully grow heteroepitaxial TiO₂ films of the rutile and anatase phases. The highest-quality rutile films were (100)/(0001)Al₂O₃, (101)/(11 $\bar{2}$ 0)Al₂O₃, (001)/(10 $\bar{1}$ 0)Al₂O₃, and (110)/(110)MgO. The X-ray rocking curves and RBS channeling data indicate that these films are aligned both perpendicular and parallel to the plane of the film. Distinct surface morphologies are observed for each orientation. The growth mechanisms of the (100), (101), and (001) rutile films were investigated, and the data suggests island or Volmer–Weber type growth. The (100) and (101) rutile orientations were also grown on (111)MgO and (1 $\bar{1}$ 02)Al₂O₃, respectively. (100) anatase grew on both (100)MgO and MgAl₂O₄.

Acknowledgements

The authors would like to thank R.H. Staley and D.L. Smith for electron microscopy. The contribution of the National Institute of Standards and Technology is not subject to copyright.

References

- [1] R.N. Ghoshtagore and A.J. Noreika, *J. Electrochem. Soc.* 117 (1970) 1310.
- [2] Y. Kumashiro, Y. Kinoshita, Y. Takaoka and S. Murasawa, *J. Ceram. Soc. Jpn.* 101 (1993) 514.
- [3] J.C. Parker, H.L.M. Chang, J.J. Xu and D.J. Lam, *Mater. Res. Soc. Symp.* 168 (1990) 337.
- [4] H.L.M. Chang, H. You, J. Guo and D.J. Lam, *Appl. Surf. Sci.* 48/49 (1991) 12.
- [5] Y. Gao, K.L. Merkle, H.L.M. Chang, T.J. Zhang and D.J. Lam, *Mater. Res. Soc.* 221 (1991) 59.
- [6] S. Chen, M.G. Mason, H.J. Gysling, G.R. Paz-Pujalt, T.N. Blanton, T. Castro, K.M. Chen, C.P. Fitorie, W.L. Gladfelter, A. Franciosi, P.I. Cohen and J. G. Evans, *J. Vac. Sci. Technol. A* 11 (1993) 2419.
- [7] K. Fukushima, I. Yamada and T. Takagi, *J. Appl. Phys.* 58 (1985) 4146.

- [8] K. Fukushima and I. Yamada, *Surf. Coating Technol.* 51 (1992) 197.
- [9] K. Fukushima, G.H. Takaoka and I. Yamada, *Jpn. J. Appl. Phys.* 32 (1993) 3561.
- [10] J.M. Bennett, E. Pelletier, G. Albrand, J.P. Borgogno, B. Lazarides, C.K. Carniglia, R.A. Schmell, T.H. Allen, T. Tuttle-Hart, K.H. Guenther and A. Saxer, *Appl. Opt.* 28 (1989) 3303.
- [11] D.R. Burgess, P.A. Morris Hotsenpiller, T.J. Anderson and J.L. Hohman, *J. Crystal Growth* 166 (1996) 763.
- [12] T.M. Graettinger, P.A. Morris, A. Roshko, A.I. Kingon, O. Auciello, D.J. Lichtenwalner and A.F. Chow, *Mater. Res. Soc. Symp.* 341 (1994) 265.
- [13] J.D. Dana and E.S. Dana, *The System of Mineralogy* (Wiley, New York, 1944) p. 554.
- [14] J.B. Goodenough, A. Hamnett, G. Huber, F. Hulliger, M. Leib, S.K. Ramasesha and H. Werheit, in: *Landolt-Börnstein, Numerical Data and Functional Relationships in Science and Technology*, Vol. 17, Subvol. g, Eds. K.-H. Hellwege and O. Madelung (Springer, New York, 1984) ch. 9.15.2.1, p. 133.
- [15] D. Wicaksana, A. Kobayashi and A. Kinbara, *J. Vac. Sci. Technol. A* 10 (1992) 1479.
- [16] H. Tang, K. Prasad, R. Sanjines, P.E. Schnid and F. Levy, *J. Appl. Phys.* 75 (1994) 2042.
- [17] K. Fukushima and I. Yamada, *J. Appl. Phys.* 65 (1989) 619.
- [18] M.B. Lee, M. Kawasaki, M. Yoshimoto, B.K. Moon, H. Ishiwaru and H. Koinuma, *Jpn. J. Appl. Phys.* 34 (1995) 808.